UNIVERSITY OF ATHENS
Faculty of Geology and Geoenvironment
Laboratory of Seismology

Institute of Geodynamics,
National Observatory of Athens

Second European Conference on Earthquake Engineering and Seismology
Istanbul August 24-29, 2014

A joint event of the
15th EUROPEAN CONFERENCE ON EARTHQUAKE ENGINEERING &
34th GENERAL ASSEMBLY OF THE EUROPEAN SEISMOLOGICAL COMMISSION

THE MAY – JULY 2013, SEISMICITY CLUSTER AT THE WESTERN CORINTH RIFT, CENTRAL GREECE

Gerasimos CHOULIARAS[1], Ioannis KASSARAS[2], Vasileios KAPETANIDIS[1],
Panagiota PETROU[1], George DRAKATOS[1] and Konstantinos MAKROPOULOS[2]

[1] *Institute of Geodynamics, National Observatory of Athens, Greece, g.choul@noa.gr*
[2] *Laboratory of Seismology, National & Kapodistrian University of Athens, Greece, kassaras@geol.uoa.gr*

Abstract
On May 21st , 2013, a large series of small earthquakes initiated a cluster formation, few km to the southeast of the city of Aigion, on the southwestern coast of the Gulf of Corinthin Central Greece. Over the next ten days more than 250 shocks with M<3.4 had been reported and on May 31st a M=3.7 earthquake was strongly felt and was accompanied by more than 100 smaller shocks within a 24 hour period. On July 13th-14th another outburst was reported with the occurrence of four M3-3.5 events, followed by more than 250 earthquakes for the next three days. Thereafter, the activity diminished and terminated in the beginning of August.
This unexpected phenomenon alarmed the local citizens because the seismic history of the area involves the occurrence of the great earthquake of 373 B.C, which extinguished the ancient city of Heliki, as described in great detail by Aristotelis in 330 B.C. The recent seismic history of the region has indicated that the Gulf of Corinth produces significantly high strain rates and it is ranked as the 'fastest' continental rifts in the world and the most seismically active part of the Mediterranean.
After the most recent catastrophic earthquake in 1995 with Ms=6.2 to the north of Aigion city, several seismological and geophysical networks have investigated the area and these have provided valuable scientific information concerning the regional seismotectonic regime. Shortly after the initiation of the May 21st, 2013 activity in Aigion, a local network of 9 portable seismographic stations was installed in the area, by the Institute of Geodynamics of the National Observatory of Athens and the Seismological Laboratory of the National Kapodistrian University of Athens. This network has been transmitting real-time data to the Hellenic Unified Seismological Network and recorded about 1000 events significantly improving the detectability of local earthquakes and the associated seismic hazard evaluation.
In this study we investigate the dynamics and spatio-temporal characteristics of the sequence. For this purpose we performed relocation of the whole sequence using catalogue and waveform data and an optimized velocity structure, which improved the initial hypocentral solutions by the order of a magnitude. A large number of focal mechanisms was computed using P-wave first motion polarities of the local recordings, implying for E-W normal faulting, compatible with regional tectonics. Furthermore, we employed a scheme involving the temporal frequency-magnitude and stress field distribution aiming to interpret the causative and triggering mechanism of the activity.

Keywords: Seismicity; Double-difference location Stress inversion; Continental rifting; Corinth gulf

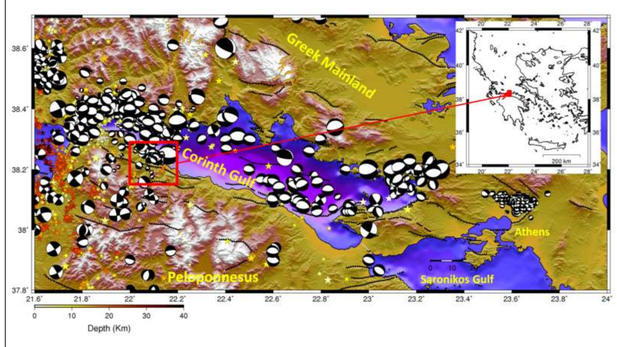

Fig 1. Map of the main tectonic features of the Corinth Gulf that includes epicenters of instrumentally recorded earthquakes with Ms≥3.0 and available focal mechanisms. The red rectangle shows the position of the study area.

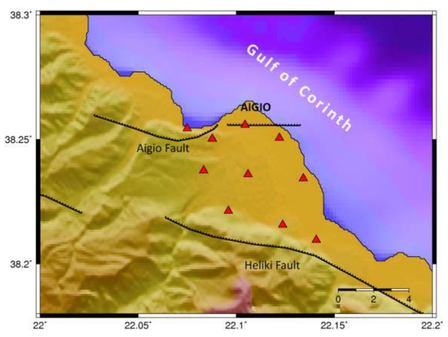

Fig 2. Map of the local seismological network which recorded the major part of the activity (after 4 June 2013) and the major faults in the area.

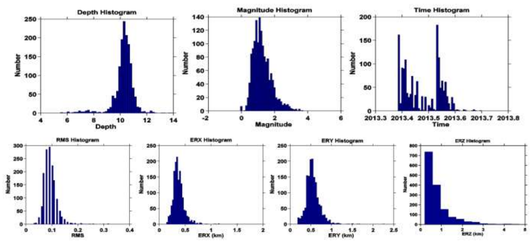

Fig 3. Histograms showing the depth, magnitude, time and error distribution of the events initially located with Hypoinverse.

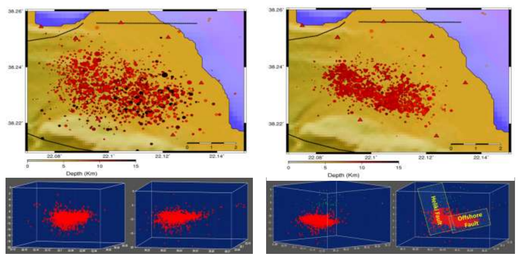

Fig 4. Spatial distribution of the 2013 Aigion cluster initially located with Hypoinverse (left) and HypoDD (right).

1. Introduction

The Corinth Gulf is one of the most seismically active zones in Europe and it is a prevailing extensional structure within the Aegean region (Fig. 1). Extension in the Aegean Sea is caused both by gravitational instability of the previous mountain belt (Hellenides) and by thinning of the lithosphere in the back arc region (Doutsos et al. 1988). Deformation throughout the Aegean is fast (~40 mm/year) progressively migrating to the south (McClusky et al. 2000). Morphotectonic and GPS observations outline the extension rate in the N185^0 direction, equal to about 11 mm yr^{-1} in the central part of the rift, reaching 16 mm yr^{-1} in the western part near Aigion. Such high strain rates constitute the Gulf of Corinth one of the fastest continental rifts in the world, an ideal 'natural' laboratory for studying extensional continental seismogenic processes.
The Corinth Rift is one of the most recent structures initiated about 1My ago (Armijo et al. 1996). As active tectonics indicate, the western part of the Gulf of Corinth is dominated by major active onshore and offshore normal faults in an approximate E-W direction. A general uplift throughout the area has lead to the formation of new faults, i.e. the well known Aigion and Helike faults (Fig. 2).
The most recent significant event in the western part of the Corinth Rift, occurred on the northern coast across from the city of Aigio on 15 June 1995 (Bernard et al., 1997). After this earthquake, the scientific results from national and international collaborative projects yielded valuable information on the seismotectonics of the region

Mostly all of the seismic activity surrounding the city of Aigio is concentrated in the western and northern parts of the Gulf, however on the southern side where the 20 km long Heliki fault lies, there has been an absence of large earthquakes since the large 1861 and 1888 events. Instrumentally recorded seismicity of this area is restricted to frequent microseismic activity. This kind of activity has been extensively monitored in the last years by local seismographic networks and it has been attributed to a crustal fluid intrusion mechanism and therefore characterized as swarm activity (e.g. Bernard et al., 2006).
On May 21, 2013, a series of small earthquakes initiated an onshore cluster formation, a few km to the southeast of the city of Aigion. More than 130 shocks of M<3 were reported within 24 hours and the associated earthquake sounds produced unrest in the local population due to the recent memories from the 1995 catastrophic earthquake and the historical citing on the sinking of the ancient city of Heliki due to the 373 B.C., M=7.3, earthquake and associated tsunami. The May-July, 2013 earthquake sequence produced a cluster of more than 1600 earthquakes of M<3.7.
In order to improve the detectability of the earthquakes during the 2013 Aigion sequence and to contribute to the assessment of the seismic hazard, a network of nine portable seismographic stations was installed locally on 4 June 2013, by the Institute of Geodynamics of the National Observatory of Athens (GI-NOA) and the Seismological Laboratory of the University of Athens (SL-UoA). The temporary acquisition deployment comprises five REFTEK-72A 24 bits digitizers equipped with Lennartz 3D/1Hz and Guralp CMG40T 1Hz seismometers and four Geotech-SMART24 digitizers equipped with Lennartz LE3D-20sec seismometers.

2. Location and HypoDD relocation

During May-August 2013, 1500 events with M<3.7 were recorded and were initially located with the use of Hypoinverse algorithm and a custom velocity model. The latter was determined with VELEST (Kissling 1988) by employing a subset of 800 best located events. Fig. 3 presents the depth, magnitude, time and error distribution of the events initially located with Hypoinverse. The detailed analysis of earthquake occurrence and fault interaction requires the accurate knowledge of the precise spatial location of earthquake hypocenters. In order to improve the hypocentral locations we applied the double-difference relocation procedure using the HypoDD algorithm (Waldhauser and Ellsworth, 2000) with both catalogue and cross-correlation differential travel-time data. Before preparing the data for relocation, we re-calculated the distance re-weighting parameters and determined a local velocity model by minimizing the RMS errors, while also reducing horizontal and vertical location errors. Following this, we applied a cross-correlation on the vertical recordings of events in four of the closest HUSN stations and created a combined cross-correlation matrix by the maximum values for each event pair. Using a nearest-neighbor linkage algorithm on the matrix data, we grouped the events with similar waveforms into multiplets with a threshold value Cth=0.85 as determined by the empirical rule of Kapetanidis and al. (2010).

This method of analysis resulted in 115 multiplets containing 80% of the recorded earthquake events. For each event pair in every multiplet and for every station within a 100 km radius, the P- or S-waves were cross-correlated separately, after being aligned on their manually picked arrival-time. Maximum cross-correlation values C (used as weights) as well as their corresponding time-lag are a vital input for HypoDD, along with travel-time data. Because of the lack of local network datafor the initial part of the sequence, the HUSN-NOA database was used and 98%of events were successfully relocated.
Figure 4 indicates the results of the location-relocation procedure which map the seismic activity onshore, 5 km to the southeast of the city of Aigio. This activity is mainly concentrated in a 3x2 km² cluster, which is oriented in a ~N100°E direction. Cross-sections of Fig. 4 show that the initially located hypocenters of the sequence form a cluster, at a focal depth range between 9.2 and 11.5 km. The relocated hypocenters appear more densely clustered on a shallow south dipping zone. Foci located at the southernmost part are concentrated on a steeper surface, which, when extrapolated to the surface, coincides with the Heliki fault trace. However, as far as the data is distributed in a narrow band, an apparent dip cannot be resolved and thus only a hypothetical association with mapped structures can be inferred.

3. Focal mechanisms

The local network geometry and station spacing allowed for the determination of 638 fault plane solutions using P-wave first-motion polarities. Concerning the recordings of the local network, P-wave onset directions were manually observed and registered. First-motion polarity observations available from the HUSN were also incorporated. Following, equal area projections of the lower hemisphere were constructed. Focal mechanism solutions were constrained by at least 10 P-wave first motions. Take-off angles were computed based on the new custom seismic velocity model. The quality of the polarity readings and the azimuthal coverage on the focal sphere were also taken into consideration.
Fig. 5 presents the spatial distribution of the 638 computed focal mechanisms across the seismogenic area. Focal mechanisms are plotted with respect to their rake and the faulting style is characterized according to the Zoback's (1992) classification scheme. As it can be observed, the majority of focal mechanisms exhibit normal faulting, while a significant number of trust and oblique slip faulting is observed at the west and east parts of the cluster. A few trust focal mechanisms are also observed at the eastern termination of the seismogenic zone. As soon as focal mechanisms concern events recorded to at least 10 stations, small events are excluded from the analysis and two spatial clusters can be now distinguished, both trending ~N100^0 (Fig. 5).

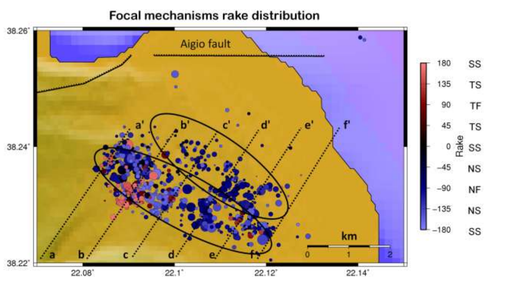

Fig 5. Map of 638 hypocenters for which focal mechanisms were computed, color coded by faulting style according to the classification scheme of Zoback (1992). Ellipses denote two spatial clusters possibly related with two conjugate antithetic faults. Dotted lines correspond to the cross-section profiles of Fig. 6.

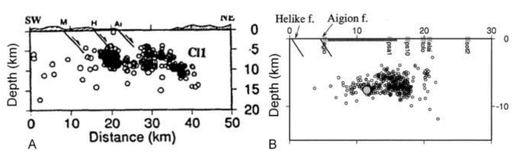

Fig. 7. Vertical cross-section at a N10^{0}E direction including (A) the July 1991 microseismicity; H: Helike fault, Ai: Aigion fault (after Rigo et al., 1996). (B) the aftershocks of the 1995 M6.5 Aigio earthquake. Small shaded dot denotes the hypocenter of the 1995 main aftershock. Active faults observed at the surface have been extrapolated to depth with a dip of 50^0 (after Bernard et al., 1997).

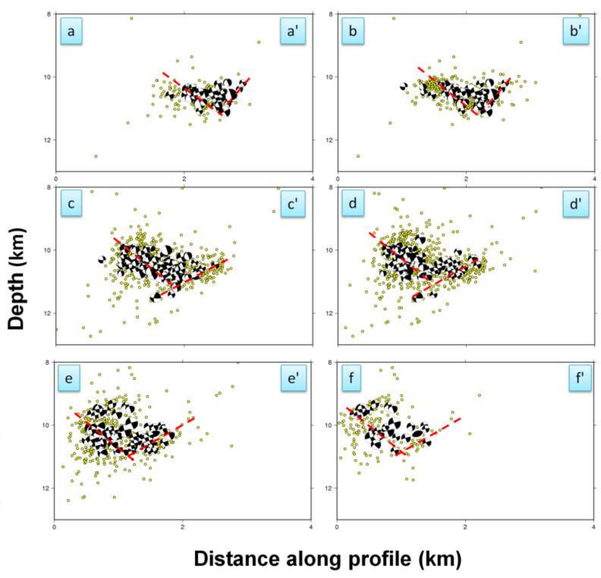

Fig 6. Cross-sections including hypocenters and focal mechanisms for events with M≥1.8, along 6 profiles (Fig. 5), perpendicular to the strike of the delineation trend of the epicenters distribution. The red dashed lines denote possible suggested faults inferred by the hypocenteral location and the focal mechanism patterns.

Cross-sections were performed perpendicular to the inferred strike of the seismogenic zone at almost N110^0 (Fig. 6). For clarity reasons, only focal mechanisms of events with M≥1.8 are included in the cross-sections. If taking into account both the foci and the nodal planes distribution, two antithetic faults are inferred. If this is the case, both faults were active during the whole period. Regarding the geometry of the fault planes, as it is also inferred from the individual fault plane solutions, the north dipping plane is steeper than the south dipping one. When extrapolated to the surface, the first coincides with the Heliki fault; the second is located offshore, north of Aigio city.
The 2013 seismic sequence resembles a similar earthquake sequence that occurred in July 1991 that produced a seismic cluster in approximately the same location (Rigo et al., 1996). Fig. 7A presents a cross section at the same area with the same direction as the ones of Fig. 6. The main cloud of hypocenters is likely related with Heliki fault, while northern, a shallow dipping seismic zone is defined, similar to the inferred pattern from our analysis. The latter, is the offshore normal fault which generated the 1995 M6.5 destructive Aigio earthquake (Bernard et al., 1997) (Fig. 7B).

4. Stress field inversion

McKenzie (1969) proposed that the crustal stress tensor cannot be estimated with confidence from the focal mechanism of one earthquake. In this preliminary investigation of the local stress field associated with the study area, we determine the best-fit stress tensor, from the set of 638 well constrained focal mechanisms by application of the inversion technique of Michael (1987, 1991). Using the statistical method of bootstrap re-sampling, we determine the 95% confidence limits of the three principal stress axis, i.e. P/S_1-axis, B/S_2-axis and T/S_3-axis and also the scalar parameter φ, which describes the relative magnitudes of the principal stresses and constrains the shape of the deviatory stress ellipsoid. Faulting characterization is consistent with Zoback (1992) and the plunge values of the P, B, and T-axis (σ_1, σ_2, and σ_3 axis) are used to assign the appropriate stress regime. Fig. 8 presents the inversion of the stress tensor associated with the May-July, 2013 seismic activity which demonstrates a very low variance and a good fit to the data, suggesting a rather homogeneous stress field and relatively coherent stress directions across the region. The determined Phi value is characteristic of a normal fault in a N100^0 direction accumulating a rather significant component of horizontal motion. The S_3/T axis indicates extension in a N357^0 direction.
Stress field inversion results are mapped in Fig. 9. The main type of faulting is normal and this is observed mainly at the central part of the seismogenic zone. Strike-slip and reverse faulting is observed at the east and west boundaries of the activated area, probably related with stress redistribution during the second phase of activity. Moreover, the larger variance (10%) of the stress field is also observed at the east and west margins of the epicentral area. The above discrepancy may possibly be related to the interaction of antithetic faults crosscutting at 9-10 km depth (Fig. 6).

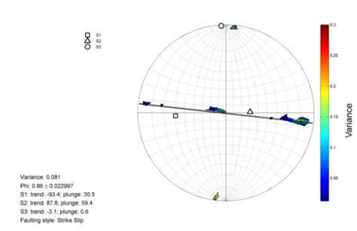

Fig. 8. Stereographic projection of the inverted stress tensor using 638 focal mechanisms computed in this study.

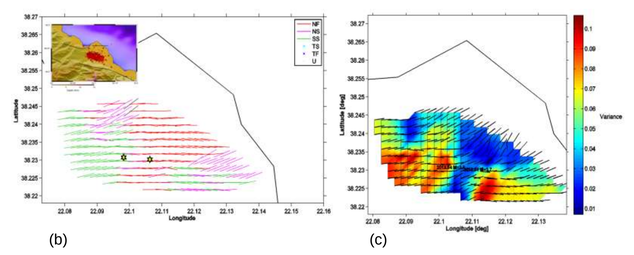

Fig. 9. Left: Map of stress inversion results using 638 focal mechanisms. Bars indicate the orientation of S_1 obtained from stress tensor inversion of focal mechanisms within 1 km radius of each node of a grid spaced 0.2×0.2 km^2. The color of bars denotes the predicted type of faulting, as displayed in the embedded legend; NF: Normal, NS: Normal Strike-slip, SS: Strike-slip, TS: Thrust Strike-slip, TF: Thrust, U: Undefined. Right: Variance of the stress tensor inversion at each node, which is a measure of the heterogeneity of the stress field.

5. Spatio-temporal characteristics of the 2013 sequence

To investigate the evolution of the spatial distribution of the cluster, the daily seismicity is analyzed accordingly (Fig.10a). Two major phases are apparently indicated: Phase A, from 21 May until 12 July 2013 and Phase B, from 13 July until the end of August 2013. The main peaks (bursts) of either periods occurred on 21-22/5 with 160 seismic events and 13-14/7 with 280 events, respectively. Secondary bursts during both phases are also observed. Figs 10b and 10c show the spatio-temporal distribution of the 2013 clusters. It is evident that the activity started at the eastern part of the seismogenic zone at a depth of 10 km and propagated west. The second phase was distributed exclusively at the western part of the activated zone. Figs 10d and 10e include the focal mechanisms of the largest events (M>2.5) indicate that both regions remained active during the entire period (Phase A + Phase B) and that rupture propagated from the east to the west.
Seismicity rate changes associated with the cluster formation are investigated using the NOA instrumental earthquake catalog which has a magnitude of completeness Mc ~3.1 for most of this region as reported by Chouliaras (2009). Fig. 11 presents the cumulative seismicity curve (blue curve) with M>1 for a 20 km radius around the May-June, 2013 cluster. A little over 6000 seismic events are reported in the last 50 years of instrumental seismicity and the sudden step in seismicity in 1995 is associated with the Ms=6.2 Aigio earthquake, while other strong earthquakes of smaller magnitudes (M>4.5, denoted by stars) have occurred to the north and to the west of the 2013 cluster. We further demonstrate the general absence of strong earthquakes in this region, by the red cumulative curve for all events with M>3, which shows a smoother behavior and a significantly lower number of earthquakes, not exceeding 1500 in the last 50 years. Further on, we observe a flattening of the M>3 curve after 2010, similar to that before the 1995 Aigio earthquake which was identified and reported as a case of significant precursory seismic quiescence by Zschau with the Seismolap algorithm (1995).
Fig. 12 presents the 2013 cumulative seismicity curve together with the stress field variance distribution with time, derived from the inversion of 638 focal mechanisms. It can be observed that the largest stress variance, although of small magnitude of the order of 14%, corresponds to the period between the two seismic phases (A and B). This is possibly related with a third preparatory phase involving stress redistribution, which likely triggered the migration of fracturing towards the west during phase B. Focal mechanisms of the largest events with M≥3 present a quite homogeneous pattern implying for ~EW normal faulting, whilst only at the final stage of the sequence variability is observed and the stress pattern is perturbed by strike-slip faulting.

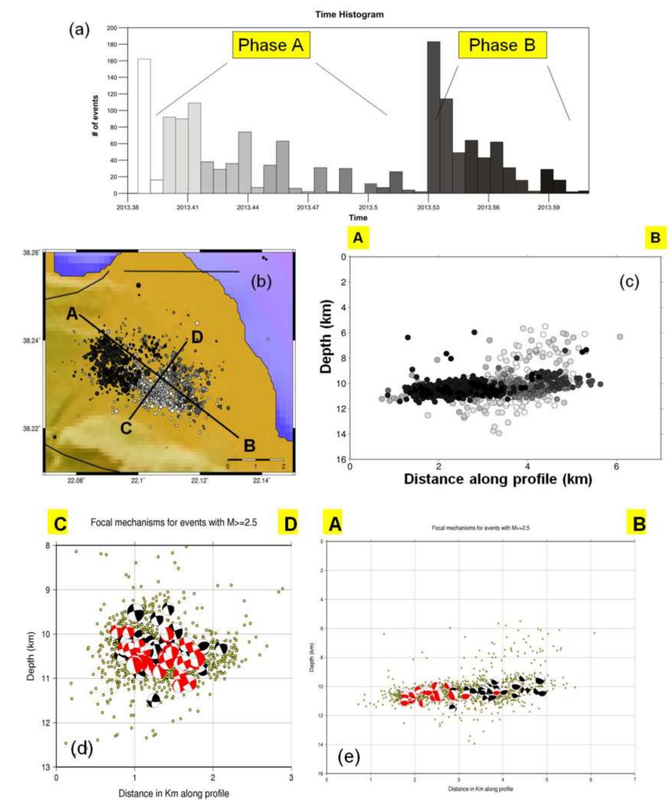

Figure 10. (a) Histogram of the temporal evolution of the seismic activity with respect to the multitude of the events; (b) Spatio-temporal distribution of the seismic activity; (c) Cross-section along strike showing the temporal distribution of the seismic activity along the seismogenic zone. The time progress is presented in grayscale, from white (for the beginning) to black (for the end of the activity); (d) Cross-section perpendicular to the strike of the seismogenic zone including focal mechanisms of events with M>2.5; (e) Cross-section along the strike of the seismogenic zone including focal mechanisms of events with M>2.5. Black quadrants of focal mechanisms: events before 13 July 2013 (Phase A); Red quadrants of focal mechanisms: events after 13 July 2013 (Phase B).

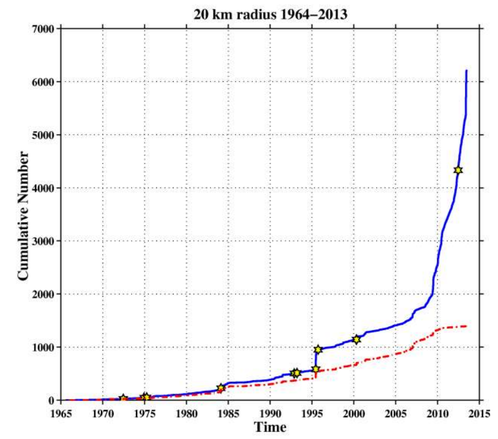

Fig. 11. Cumulative seismicity for a circular area of 20km radius around the May-July, 2013 seismic activity. Earthquakes are reported by the NOA catalog. The blue curve indicates cumulative seismicity for M>1 and the red curve for M>3. Events with M>4.5 are indicated by stars.

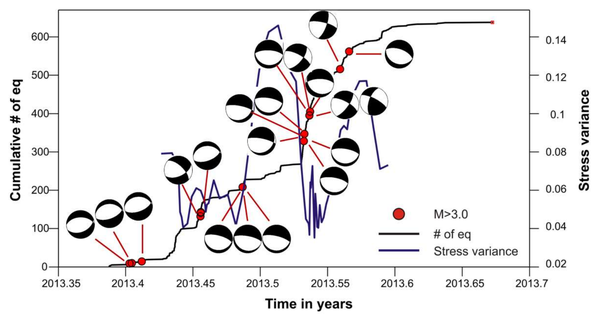

Fig 12. Tri-axial diagram comparing the cumulative seismicity and the stress field variance distribution with time. Focal mechanisms correspond to events with M>3.0.

Conclusions

1. The 2013 activity, occurred in an area of rapid continental rifting, is compatible with E-W normal faulting and N-S extension.
2. Two major seismic phases are clearly distinguished: (A) between 21 May and 12 July 2013 and (B) from 13 July until the end of August 2013.
3. Migration of fracturing towards the west is evidenced.
4. Diversity of the stress field is inferred at the boundaries of the seismogenic zone.
5. The first phase is characterized by relatively homogeneous stress pattern, responsible for E-W normal faulting.
6. During the second phase the stress field is perturbed by strike slip and reverse fracturing.
7. The largest perturbation of the stress field, of the order of 14%, is observed before the initiation of the second phase on 13/7/2013
8. The geometry of the seismogenic zone is fairly compatible with the one inferred previously during a swarm in 1991 (Rigo et al., 1996).
9. Although more analysis is needed, both relocated hypocenters and nodal planes of 638 well constrained focal mechanisms provide implications for two E-W trending antithetic normal faults. A steep north dipping plane is likely related with the major Heliki fault. The other one is a low angle south dipping plane, that was probably activated during the aftershock activity of the 1995 Ms=6.2 Aigio destructive earthquake (Bernard et al., 1997).

It is still under question whether this repeatable phenomenon is of local origin, or it is due to a larger scale mechanism responsible for the rapid regional rifting in the Corinth Gulf. In order to resolve the latter, triggering indices should be searched in the study area, involving (e.g.) fluids and/or heat convection.